Periodica Polytechnica
Mechanical Engineering

61(4), pp. 282-287, 2017
https://doi.org/10.3311/PPme.11085

Design and Analysis of 3D Printable Foot Prosthesis

Bence Rochlitz[1], Dávid Pammer[1*]

RESEARCH ARTICLE

Received 01 June 2017; accepted after revision 18 July 2017

Abstract

3D printing manufacturing process has the possibilities to produce individual medical devices, especially implants and prosthesis with short production time. The aim of this study is to design a 3D printable Energy Storage and Return (ESAR) foot prosthesis for transtibial amputees with a novel geometry. The criteria of the prosthesis were 3D printable, low cost, simply geometry and satisfying mechanical properties for low activity use. The finite element analysis of the designed foot prosthesis was conducted in each of the three support phases of the walking cycle (controlled plantarflexion, controlled dorsiflexion, powered plantarflexion or push-off phase). Besides of the simulations the prototype was printed by fused deposit modeling (FDM) technology, used ABS material and the produced prototype was investigated in quasi-static and cyclic compression. It can be stated after the investigation (simulation and test) that the 3D printed prototype fulfill the requirements and it can be used as passive ESAR foot prosthesis.

Keywords

3D printing, FDM, ABS, foot prosthesis, FEA, destructive test

[1] Department of Materials Science and Engineering
Faculty of Mechanical Engineering,
Budapest University of Technology and Economics
H-1111 Budapest, Műegyetem rkp. 3., Hungary
[*] Corresponding author, e-mail: pammer@eik.bme.hu

1 Introduction

Most commercially available foot prostheses are passive. Their materials are either carbon or glass fiber reinforced composites, which are able to store and return a sufficient amount of energy to provide propulsion. These prostheses are expensive, and the more affordable SACH (Solid Ankle Cushioned Heel) designed for patients with low activity level fails to return energy, and its stability could be improved [1]. High-energy return is a key feature of well-designed prostheses [2]. The rapid development of additive manufacturing techniques makes it possible to design 3D-printable foot prostheses that have the properties of ESAR (Energy Storage and Return) feet.

The FDM (Fused Deposit Modeling) technology has a number of benefits. The geometric freedom of the additive technology makes it possible to maximize strength and minimize weight. These parameters are also controlled by the infill pattern and with the right infill, energy storage can be boosted [3, 4].

The geometric freedom provided by 3D printing helps customize prostheses to meet the varying needs of patients. The CAD models are adjustable after testing with amputees, based on their feedback. Using this method an optimal geometry can be created for low-volume production or for individual custom prostheses.

A wide variety of materials is available as FDM filaments, including plastics with good mechanical properties. Different types of ABS and PC-ABS are often used in the industry for load-bearing parts. The energy storing nature of these plastics is beneficial for the user during the push-off phase. Carbon and glass fiber filaments are also used with FDM in order to create strong composite material parts.

In a study published in 2015, a 3D-printable foot prosthesis was designed and manufactured using PLA filament [1]. The research aimed to minimize the costs, so that the product can be printed at home, and donated to residents of developing countries. The results were appealing. However, the low heat resistance of PLA might cause excessive deformation and it is not the ideal material as far as its mechanical properties are concerned.

The aim of this study was to develop a new fairly low-cost ESAR foot with novel geometry and manufacturing technology. The design met with the additive manufacturing's design and biomechanics' criteria. The new ESAR foot was 3D printed, using FDM technology and ABS plastic. The 3D printed prosthesis gives an alternative choice for moderate activity level amputees.

2 Materials and Methods

2.1 CAD design

A number of CAD models were designed, all adjustments of the model were followed by FEA, thus optimizing its strength. The split forefoot and the heel provide a 3-point support. The front support points are positioned according to the human foot. The sides are not arched in order to provide better stability than the SACH foot [1].

The heel is robust just like the human heel. The rear rib had to be implemented due to high stress at the heel area; moreover, the heel was narrowed in order to reduce the area that is in contact with the ground.

The CAD adjustments aimed to create a low-build prosthesis so that it would fit lower amputees as well. The prototype was made for a 245 mm long foot (EU size 39) with a height of 143 mm and width of 81 mm. It corresponds to a woman's or child's foot (Fig. 1).

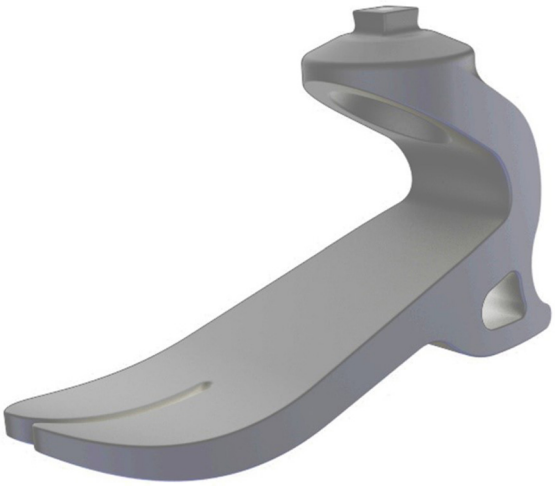

Fig. 1 The novel geometry of the designed foot prosthesis.

2.2 Materials

The design was mainly based on the human foot, and it was decided that the FDM filament would be ABSplus-P430 from Stratasys for the prototype. This filament is of 31 MPa of yield tensile strength and 2200 MPa of tensile modulus in the XZ axis (0° orientation, tested by ASTM 638 method). 58 MPa of flexural strength and 2100 MPa of flexural modulus in the XZ axis (0°orientation, tested by ASTM D790 method) and is sufficiently heat resistant with a heat deflection value of 96 °C at 4.5 bar.

2.3 FEA design and FEA testing

The FEA was conducted in each of the three support phases of the walking cycle (controlled plantarflexion, controlled dorsiflexion, powered plantarflexion/push-off phase). In every phase, the critical position of the ankle was considered [5, 6]. Moreover, the average maximum lateral load and the auxiliary torque (the load line is not aligned with the axis of the mounting pyramid) were superimposed on the vertical load (weight).

Matching the prototype's size, a person with 60 kg body mass was presumed for the FEA. The vertical load of the model was 1.5 times the person's weight (900 N). The lateral load was defined as 23% of the body weight that is 207 N [7]. The auxiliary torque was calculated at 15750 Nmm for a 900 N vertical load.

As far as the mechanical properties are concerned, the tensile strength and modulus of the ABSplus-P430 were used in the simulation. The material model was defined as linear and isotropic. FDM printed ABS plastics show quasi – linear characteristics until their yield point [8]. The geometry of the model and the material properties are more profound; however, these assumptions are solid approximations for the FEA.

2.4 3D Printing

The FEA analysis was carried out on the solid body model. However, the prototype was printed with a 30% rectangular infill pattern and a 1.5 mm wall thickness to reduce mass and printing time. It was decided that the prosthesis would be printed on its side to ensure that the fibers are continuous and aligned in the direction of the main stress. Layer resolution was set to 200 μm, and wall thickness was set to 1.5 mm. The prototype was manufactured with a Stratasys Dimension 1200es printer.

The prototype's mass was reduced to 162 grams from 544 grams because of the infill (Fig. 2). The printing time was approximately 14 hours, and it took an additional 6 hours to remove the support material.

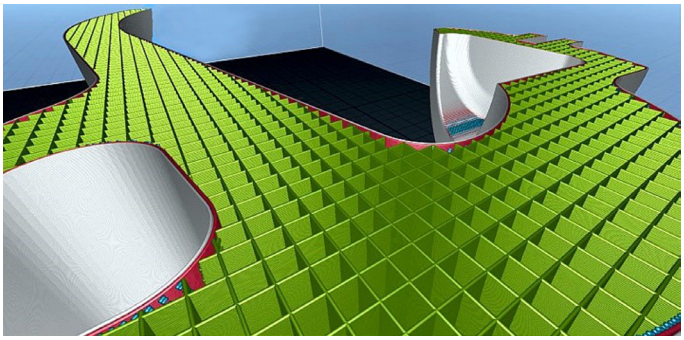

Fig. 2 The manufacturing parameter of the geometry was 30% rectangular infill pattern, 1.5 mm wall thickness and 0.2 mm layer.

2.5 Mechanical testing

The prototype was tested twice using Instron 5965 testing system. First, it was placed on its sole, without any additional support, and a 600 N vertical load was applied three times.

The loading rate was 0.5 mm/min, 1 mm/min and 1.5 mm/min respectively. During the second test, five different loads were applied in increasing order: 200 N, 400 N, 600 N, 800 N and 1000 N respectively. The loading speed was 1 mm/min, and extra support was added at the heel, thus avoiding undesired slipping that occurred during the first test. This time, data was collected throughout loading and relieving as well. By numerically integrating the two curves, and calculating their ratio in every instance, the energy returned by the prosthesis is identifiable. Fig. 3 depicts the testing arrangements.

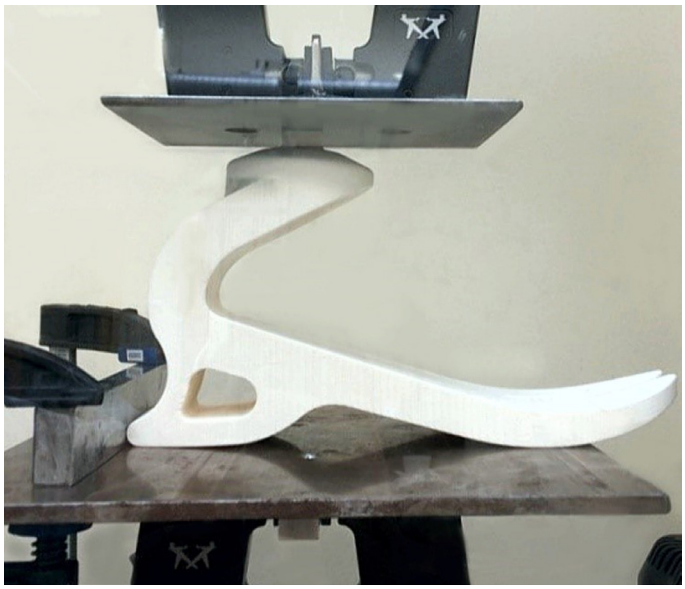

Fig. 3 The compression investigation of the prototype.

3 Results

3.1 FEA results

Heelstrike (HS) was modeled with a fixed constraint on the sole of the heel and the 900 N vertical load on the top surface of the mounting pyramid. The maximum stress was computed at 11.74 MPa on the inner side of the ankle and the maximum displacement was 2.29 mm.

In mid-stance (MS), the whole surface of the sole touches the ground. This phase was modeled with a frictionless constraint and a pin constraint on the bottom surface of the heel and the forefoot respectively. The 900 N load was applied on the top of the mounting pyramid. The maximum stress turned out to be 11.73 MPa and the maximum displacement was 2.11 mm (Fig. 4)

In the push-off phase (PO), two simulations were conducted. First, the 900 N load was placed on top of the pyramid and the forefoot's bottom surface was fixed (in order to constrain the surface, it was split). The second time, the pyramid was mounted and the vertical load was applied on the forefoot's sole. The results were different (Fig. 5), which is an indication that testing might provide more accurate information than the computer simulation.

In the first case, the maximum stress at the ankle was approximately 10 MPa. However, close to the constraint, the stress increased excessively. In the second analysis, a maximum stress of 35-36 MPa was calculated at the ankle. Therefore, further investigation is needed in this phase to accurately evaluate the strength of the prototype. In intact walking, there is a short interval before toe-off, when the other leg is already in the swing phase so that the whole body weight falls on the support leg. The FEA setups above model this interval.

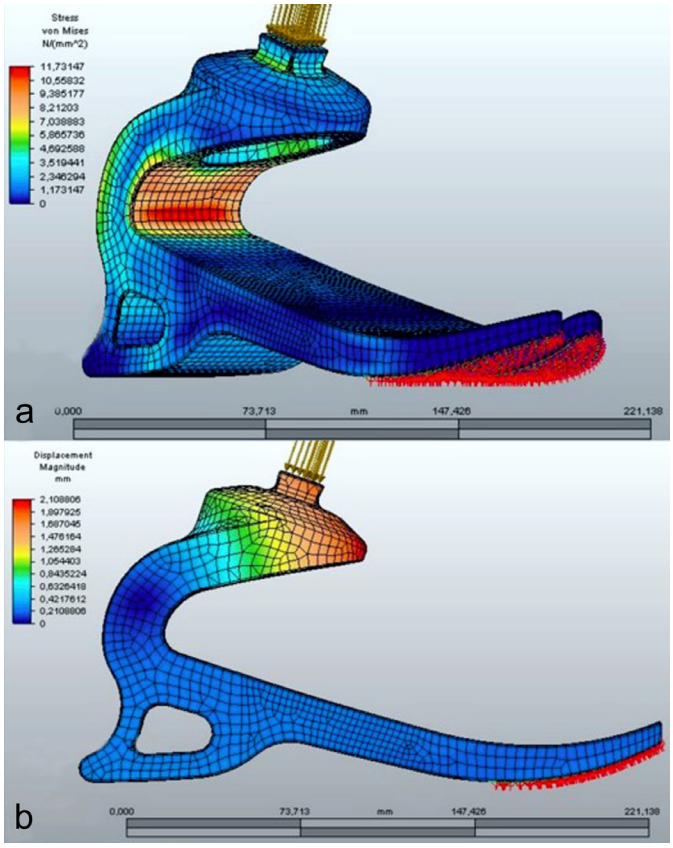

Fig. 4 Mid-stance (MS) - equivalent stress (a) and displacement state (b) at 5x magnification.

The axis of the mounting pyramid and the load line are not aligned. Therefore, an additional auxiliary torque (AT) has to be considered. This torque generates 4,8-5 MPa stress at the inner ankle area. The simulation takes place at heel strike with the torque applied on the top of the pyramid and a fixed constraint on the heel.

The inversion and eversion movements of the biological ankle may also occur while walking with the prosthesis. These forces (a lateral force-LF) are superimposed on the body weight. The corresponding maximum stress calculated with the aforementioned 23% body weight is approximately 3 MPa at the ankle area (Fig. 6). The simulation is at heel strike with the load on the top of the pyramid and a fixed constraint on the heel.

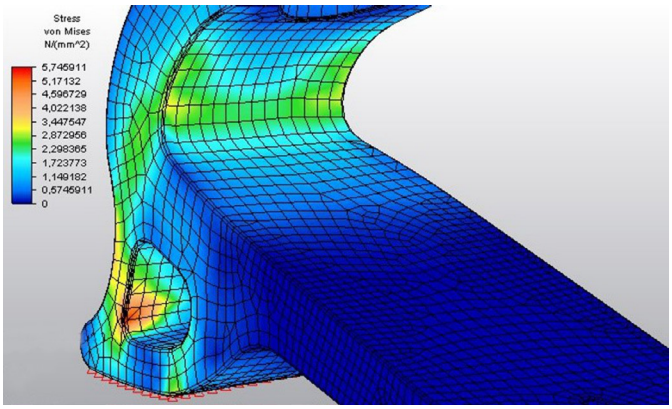

Fig. 6 Lateral force (LF) - equivalent stress state at 5x magnification.

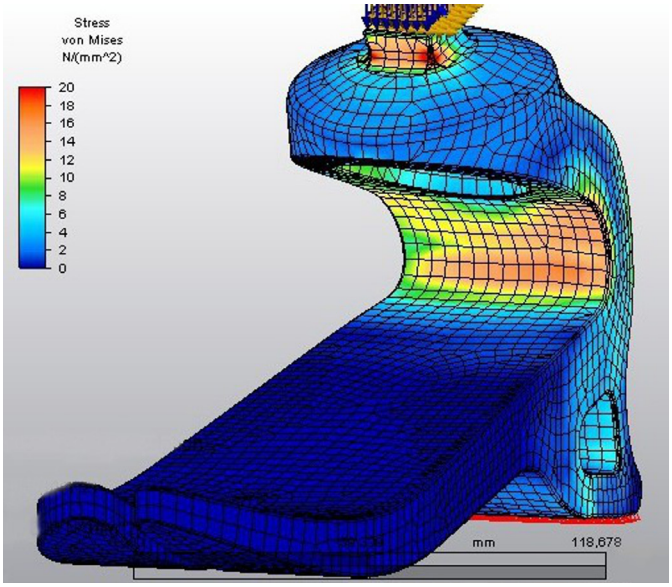

Fig. 7 Equivalent stress state of the summarized auxiliary torque (AT) and lateral force (LF) at 5x magnification.

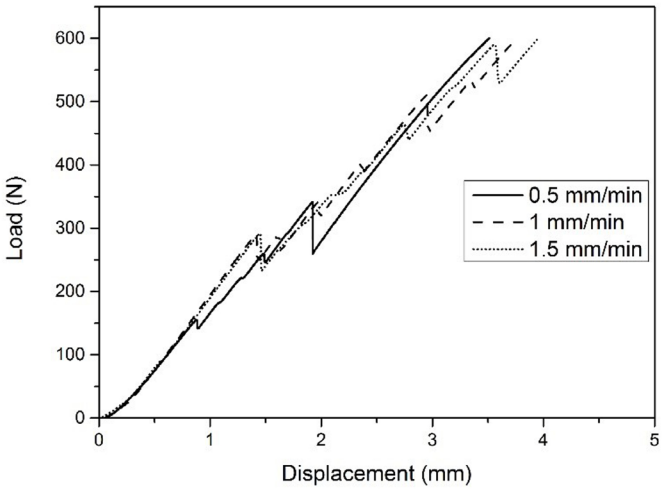

Fig. 8 The quasi-static compression test curves with slipping parts.

In Table 1 all the results can be found. In the last column, HS total means that the auxiliary torque and the maximum lateral force were superimposed on the vertical load in the simulation. The results are given in Fig. 9.

Table 1 The simulation results of walking cycle's phases

	HS	MS	PO
Load (N)	900	900	900
Max stress of ankle (MPa)	11.74	11.73	10…36
	AT at HS	LF at HS	HS total
Load (N)	15750	207	*
Max stress of ankle (MPa)	5	3	17

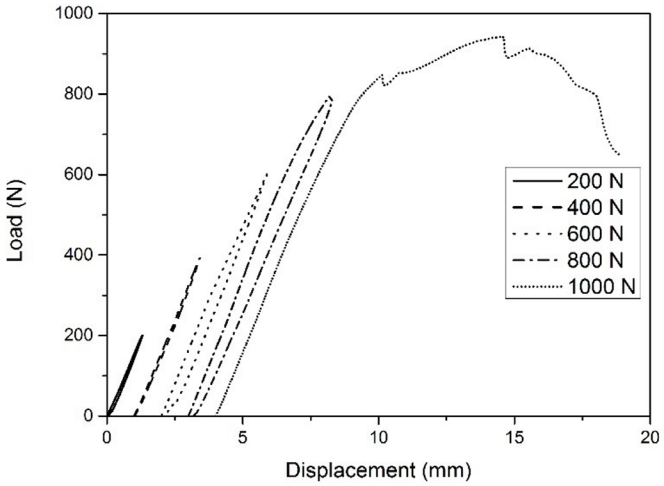

Fig. 9 Incremental cyclic compression test curves, and the failure state.

3.2 Test results

The load – displacement diagram is shown for the 600 N maximum load, applied with different speeds. The curves are quasi – linear meaning that the weight is within the elastic deformation range. The ankle geometry of the prosthesis generates a torque that wants to rotate it forward. Because of that and the lack of lateral support, the prosthesis kept slipping frequently, which resulted in non-continuous curves. This phenomenon shows that the prosthesis is able to push its user forward, and that is a beneficial feature.

The second test is displayed for 200 N, 400 N, 600 N, 800 N and 1000 N maximum loads. The strain axes of the graphs are adjusted by 0, 1, 2, 3 and 4 mm respectively so that all of them are visible. As it can be seen, the prototype failed at approximately 850 N and the yield point is at approximately 750 N.

Failure was anticipated around this amount of load, because the prototype was weakened by the infill, compared to the solid model. Seconds before failure, the foot started cracking which was audible. The rear area of the sides was thrust outwards, while the front area in the opposite direction and that caused the break (see Fig. 10).

The area of the hysteresis loop was calculated by numerically integrating the upper and lower curves in each of the first four cases. That area corresponds to the dissipated energy. The returned energy for each load is shown in Table 2. The average of the four values is 88% with a corrected standard deviation of 5.1%.

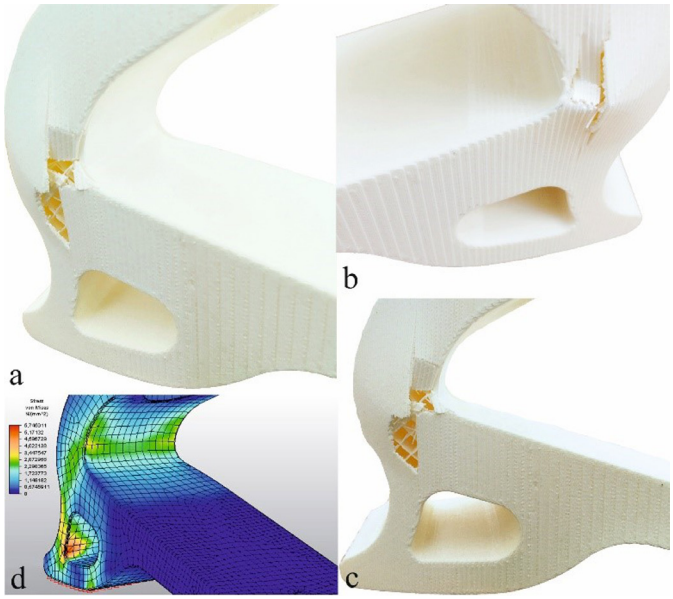

Fig. 10 The damaged protoype (a, b and c) and the similar simulated critical zones.

Table 2 Returned energy in all cases

Load (N)	200	400	600	800
Returned energy (%)	88.4	95	85.7	83.1

4 Discussion

The FEA conducted on the prototype with 150% of presumed body weight showed that at HS the maximum stress was 17 MPa in the critical area compared to the 31 MPa yield strength of the material. HS puts a dynamic stress on the foot, that is why 150% of the load was necessary for the calculations. In the push-off phase, more information is needed to fully evaluate the prototype. However, for low-activity patients, the toe-off phase is different than it is for high-activity users. At slower walking speeds the interval, in which one leg is raised, and the other forefoot provides the only support, does not exist. Therefore, the load on the prosthesis would be only half of the body weight, and the simulation was conducted with 1.5 times the body weight.

Considering that human feet weigh a few times more than the prototype [9], it is desirable to increase its mass in order to improve its strength and provide a more natural feeling for the user. The way to do so is adjusting printing settings such as wall thickness and infill percentage, as well as the geometry of the model, which is not optimal yet. The FEA pointed out that the middle area of the foot does not bear enough stress compared to the critical ankle area. Future work will focus on that.

Current additive manufacturing technologies allow designers to fabricate composite parts. Carbon fiber loading multiples the strength of the neat ABS plastic. With 10 wt% (weight percent) loading of the filament blend, the tensile strength of the material becomes 1.5–2 times greater, while the tensile modulus quadruples when FDM process is used [10]interest is growing in direct manufacture of actual parts. For wide spread application of 3D additive manufacturing, both techniques and feedstock materials require improvements to meet the mechanical requirements of load-bearing components. Here, we investigated short fiber (0.2\u20130.4 mm. Another technology, called Composite Filament Fabrication (CFF) makes it possible to 3D print composites with continuous fibers. MarkForged's carbon fiber and fiberglass filaments have unique strength among 3D-printable materials [11, 12]Fiberglass or Kevlar fibers. The aim of this study is to evaluate the elastic properties of the fiber reinforced 3D printed structures and predict elastic properties using an Average Stiffness (VAS. Fiber reinforcement creates an opportunity to significantly enhance the artificial limb's strength and expand its lifetime. Such materials might be used for prostheses for high activity level users.

5 Conclusion

In conclusion, the 3D-printable prosthetic foot design presented in this paper shows that such products built of ABS filament have a potential to be a low-cost solution for moderate activity level amputees. Based on the data collected during quasi-static testing, the energy return of the prosthesis is sufficient (88.0 ± 5.1%). For high activity level patients, new CFF technology will enable to 3D-print ESAR feet with greater strength.

The development of a novel 3D printed prosthesis is limited to the materials and not to the design of the prosthesis. Seeing the evolution of 3d printing materials, with time more and better materials can be chosen to print a functional end-user product.

Future work will focus on testing the prosthesis with patients and improving its strength and lifetime. As new additive manufacturing techniques and materials are available, they can be considered to be utilized in the field of foot prostheses.

Acknowledgement

The present work was funded by the National Research, Development and Innovation (NKFIH) Fund, Project title: "Developing a new generation of customized medical implants and medical aids for additive technologies"; The application ID number: NVKP_16-1-2016-0022.

References

[1] Yap, J., Renda, G. "Low-cost 3D-printable Prosthetic Foot." In: Christer, K. (ed.), *Proceedings of the 3rd European Conference on Design4Health*. Sheffield. 2015. Availabled from: http://research.shu.ac.uk/design4health/wp-content/uploads/2015/07/D4H_Yap_Renda.pdf [Accessed: 17th July 2017]

[2] Takahashi, K. Z., Stanhope, S. J. "Mechanical energy profiles of the combined ankle–foot system in normal gait: Insights for prosthetic designs." *Gait & Posture*. 38(4), pp. 818–823. 2013. https://doi.org/10.1016/j.gaitpost.2013.04.002

[3] Thorpe, C. T., Klemt, C., Riley, G. P., Birch, H. L., Clegg, P. D., Screen, H. R. C. "Helical sub-structures in energy-storing tendons provide a possible mechanism for efficient energy storage and return." *Acta Biomaterialia*. 9(8), pp. 7948–7956. 2013. https://doi.org/10.1016/j.actbio.2013.05.004

[4] Abueidda, D. W., Bakir, M., Abu Al-Rub, R. K., Bergström, J. S., Sobh, N. A., Jasiuk, I. "Mechanical properties of 3D printed polymeric cellular materials with triply periodic minimal surface architectures." *Materials & Design*. 122, pp. 255–267. 2017. https://doi.org/10.1016/j.matdes.2017.03.018

[5] Au, S. K., Weber, J., Herr, H. "Biomechanical Design of a Powered Ankle-Foot Prosthesis." In: 2007 IEEE 10th International Conference on Rehabilitation Robotics. Noordwijk, 2007, pp. 298-303. https://doi.org/10.1109/ICORR.2007.4428441

[6] Versluys, R., Beyl, P., Van Damme, M., Desomer, A., Van Ham, R., Lefeber, D. "Prosthetic feet: state-of-the-art review and the importance of mimicking human ankle-foot biomechanics." *Disability and Rehabilitation: Assistive Technology*. 4(2), pp. 65–75. 2009. https://doi.org/10.1080/17483100802715092

[7] Major, M. J., Twiste, M., Kenney, L. P. J., Howard, D. "Amputee Independent Prosthesis Properties—A new model for description and measurement." *Journal of Biomechanics*. 44(14), pp. 2572–2575. 2011. https://doi.org/10.1016/j.jbiomech.2011.07.016

[8] Szykiedans, K., Credo, W. "Mechanical Properties of FDM and SLA Low-cost 3-D Prints." *Procedia Engineering*. 136, pp. 257–262. 2016. https://doi.org/10.1016/j.proeng.2016.01.207

[9] Ma, Y., Kwon, J., Mao, Z., Lee, K., Li, L., Chung, H. "Segment inertial parameters of Korean adults estimated from three-dimensional body laser scan data." *International Journal of Industrial Ergonomics*. 41(1), pp. 19–29. 2011. https://doi.org/10.1016/j.ergon.2010.11.004

[10] Tekinalp, H. L., Kunc, V., Velez-Garcia, G. M., Duty, C. E., Love, L. J., Naskar, A. K., Blue, C. A., Ozcan, S. "Highly oriented carbon fiber–polymer composites via additive manufacturing." *Composites Science and Technology*. 105, pp. 144–150. 2014. https://doi.org/10.1016/j.compscitech.2014.10.009

[11] Markforged Inc. "MarkForged develops 3D printer for carbon fibre." *Reinforced Plastics*. 59(1), p. 12. 2015. https://doi.org/10.1016/j.repl.2014.12.027

[12] Melenka, G. W., Cheung, B. K. O., Schofield, J. S., Dawson, M. R., Carey, J. P. "Evaluation and prediction of the tensile properties of continuous fiber-reinforced 3D printed structures." *Composite Structures*. 153, pp. 866–875. 2016. https://doi.org/10.1016/j.compstruct.2016.07.018